Dynamics of Biofilm Processes
Author(s): Michael G. Trulear and William G. Characklis
Source: *Journal (Water Pollution Control Federation)*, Vol. 54, No. 9, Annual Conference Issue (Sep., 1982), pp. 1288-1301
Published by: Water Environment Federation
Stable URL: http://www.jstor.org/stable/25041684
Accessed: 27-10-2017 20:17 UTC

Dynamics of biofilm processes

Michael G. Trulear, William G. Characklis

Biofilms can develop on almost any surface exposed to an aqueous environment. The biofilm systems that result can be used beneficially, as exemplified by fixed-film wastewater treatment processes (for example, trickling filters and rotating biological contactors). In addition, biofilms play a major positive role in stream purification processes. However, biofilms can be quite troublesome in certain engineering systems. In water distribution systems and heat transfer equipment, for example, biofilms can cause substantial energy losses resulting from increased fluid frictional resistance and increased heat transfer resistance. The significance of biofilm development on various processes is summarized in Table 1.

PROCESSES CONTRIBUTING TO BIOFILM DEVELOPMENT

Biofilm development on a surface exposed to a fluid flow is the net result of several physical, chemical, and biological processes including the following:

- Transport and adsorption of organic molecules to the surface,
- Transport of microbial cells to the surface,
- Microorganism attachment to the surface,
- Microbial transformations (growth and exopolymer production) at the surface resulting in the production of biofilm, and
- Partial detachment of the biofilm caused by fluid shear stress.

The *adsorption* of an organic monolayer occurs within minutes after exposure of an initially "clean" surface to a flowing fluid that contains dispersed microorganisms, nutrients, and organic molecules. Baier[1-4] has investigated the dynamics of this organic adsorption and suggests that such adsorption is a prerequisite for biological attachment because it conditions the surface. The *transport* of microbial cells from the bulk to the surface depends on the fluid flow regime. In turbulent flow, molecular diffusion and turbulent eddy transport are viable mechanisms. In a quiescent fluid, chemotaxis is possible.

Numerous mechanisms have been postulated for the process of microbial *attachment* to the surface.[5,6] Most agree that the production of a polysaccharide binding material is necessary. Biofilm *production* is the combined effect of cellular reproduction and extracellular polymer production. The rate of biofilm production depends on the diffusion of nutrients into the biofilm followed by their synthesis into attached biomass. Nutrient or oxygen depletion in lower layers of the biofilm can significantly limit the overall production process.

Rate expressions have been developed for substrate removal and biofilm accumulation and detachment.

At any point in the development of a biofilm, portions of biofilm are sheared away and re-entrained in the fluid flow. *Detachment*, a continuous biofilm removal process, is highly dependent on hydrodynamic conditions. In addition to shearing, sloughing also can significantly contribute to detachment. Sloughing refers to a random, massive removal of biofilm attributed to nutrient/oxygen depletion deep within biofilms. Sloughing is more frequently witnessed with thicker, less dense films that develop under low fluid shear conditions.

Biofilm accumulation is the net result of all these rate processes occurring simultaneously (Figure 1). At specific times in the overall biofilm development, certain processes contribute more than others.

The objectives of this research were

1. To determine the effect of substrate loading and fluid velocity on the processes associated with biofilm accumulation, and
2. To determine the influence of biofilm accumulation on fluid frictional resistance.

APPARATUS AND METHODS

An annular reactor constructed of acrylic plastic and consisting of two concentric cylinders, a stationary outer cylinder and a rotating inner cylinder, was used in this study. Figure 2 illustrates details of the reactor. Rotational velocity was electronically controlled and continuously displayed. A torque transducer mounted on the shaft between the rotating cylinder and the motor drive was monitored continuously and displayed changes in fluid frictional resistance caused by microbial film development. A thin removable slide, which formed an

Table 1—Effect and relevance of biofilms on various rate processes.

Effects	Specific process	Concerns
Heat transfer reduction	Biofilm formation on condenser tubes and cooling tower fill material. *Energy losses.*	Power industry Chemical process industry U. S. Navy Solar energy systems
Increase in fluid frictional resistance	Biofilm formation in water and wastewater conduits as well as condenser and heat exchange tubes. Causes increased power consumption for pumped systems or reduced capacity in gravity systems. *Energy losses.*	Municipal utilities Power industry Chemical process industry Solar energy systems
	Biofilm formation on ship hulls causing increased fuel consumption. *Energy losses.*	U. S. Navy Shipping industry
Mass transfer and chemical transformations	Accelerated corrosion caused by processes in the lower layers of the biofilm. Results in *material deterioration* in metal condenser tubes, wastewater conduits, and cooling tower fill.	Power industry U. S. Navy Municipal utilities Chemical process industry
	Biofilm formation on remote sensors, submarine periscopes, sight glasses, and so on, causing *reduced effectiveness.*	U. S. Navy Water quality data collection
	Detachment of microorganisms from biofilms in cooling towers. Releases *pathogenic organisms* (for example, *Legionella* in aerosols).	Public health
	Biofilm formation and detachment in drinking water distribution systems. Changes *water quality* in distribution system.	Municipal utilities Public health
	Biofilm formation on teeth. Causes *dental plaque and caries.*	Dental health
	Attachment of microbial cells to animal tissue. Causes *disease* of lungs, intestinal tract, and urinary tract.	Human health
	Extraction and oxidation of organic and inorganic compounds from water and wastewater (for example, rotating biological contacters, biologically aided carbon adsorption, and benthal stream activity). *Reduced pollutant load.*	Wastewater treatment Water treatment Stream analysis
	Biofilm formation in industrial production processes *reduces product quality.*	Pulp and paper industry
	Immobilized organisms or community of organisms for conducting *specific chemical transformations.*	Chemical process industry

integral fit with the inside wall of the outer cylinder, was used to determine biofilm thickness and biofilm density. The reactor was completely mixed by virtue of the pumping action of four draft tubes and an impeller mounted at the bottom of the inner cylinder.[7] Table 2 presents relevant characteristics and dimensions of the reactor. Advantages of the annular configuration included the following:

- Because of complete mixing, no concentration gradients existed in the bulk fluid; this factor simplified mathematical descriptions and sampling;
- Fluid shear stress at the wall could be varied independently of mean residence time; and
- There was high surface-area-to-volume ratio.

The reactor feed consisted of substrate solution plus treated dilution water. The substrate solution was composed of glucose as the sole carbon and energy source plus micronutrients and phosphate buffer (Table 3). The concentrations of micronutrients were in the same proportions as used by Kornegay and Andrews.[7] The 0.008 M phosphate buffer was sufficient to maintain the reactor pH at 7.0 ± 0.1. The dilution water to the reactor was tap water that had been treated to remove suspended solids along with residual chlorine and sol-

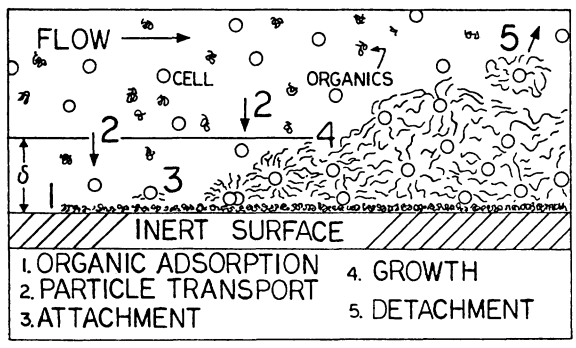

Figure 1—Processes contributing to biofilm development.

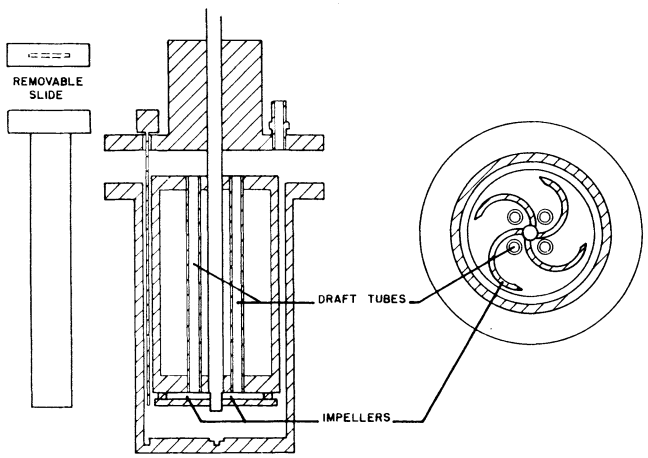

Figure 2—Schematic diagram of annular reactor.

uble organics. The substrate solution and dilution water were continuously fed into the reactor by peristaltic pumps. Prior to entering the reactor, dilution water passed through a temperature adjustment reservoir that maintained reactor temperature at 30 ± 0.5°C.

Prior to temperature adjustment, the dilution water was held in a plastic storage container (15 l), where it was continuously aerated to provide a dissolved oxygen (DO) concentration near saturation in the reactor influent. Reactor effluent DO concentration was periodically measured with a DO probe to ensure that aerobic conditions were maintained in the reactor solution.

The thickness of microbial film was determined with the stage micrometer of a microscope in a method adapted from that of Sanders.[8] The removable slide was withdrawn from the reactor, placed in a vertical position for 1 minute to allow excess water to drain, and then placed on the microscope stage. The 10× objective

Table 2—Relevant characteristics and dimensions of the annular reactor.

Reactor	
Liquid volume	570 cm^3
Total wetted surface area (including draft tubes and impeller assembly)	2 000 cm^2
Inner cylinder wetted surface area (including draft tubes and impeller assembly)	1 069 cm^2
Outer cylinder wetted surface area	931 cm^2
Diameter of inner cylinder	10.5 cm
Width of annular gap	0.4 cm
Wetted height of inner cylinder	17.4 cm
Wetted height of outer cylinder	20.3 cm
Volumetric flow rate (nutrients plus dilution water)	57 cm^3/min
Mean residence time	10 min
Removable slide	
Wetted surface area	60.9 cm^2
Width	22.5 cm
Height	2.9 cm

Table 3—Composition of substrate solution.

Constituent	Conc. in dilution
$FeCl_3$	0.045 mg/l
$MnCl_2 \cdot 4H_2O$	0.011
$ZnCl_2$	0.008
$CuCl_2 \cdot 2H_2O$	0.005
$CoCl_2 \cdot 6H_2O$	0.007
$(NH_4)_6Mo_7O_{24} \cdot 4H_2O$	0.005
$Na_2B_4O_7 \cdot 10H_2O$	0.003
Na_3Citrate	0.408
$NaH_2PO_4 \cdot H_2O$	0.575
$(NH_4)_2SO_4$	0.367
NH_4Cl	3.417
$CaCl_2$	0.308
$MgCl_2 \cdot 6H_2O$	0.565
KH_2PO_4 (Buffer)	0.004 M
Na_2HPO_4 (Buffer)	0.004 M
Glucose	10 mg/l

Note—For glucose concentrations greater than 10 mg/l, the concentration of nutrient constituents was proportionately increased.

(100× total magnification) was lowered until the biofilm surface was in focus, and the fine adjustment dial setting of the stage micrometer was recorded. The objective was then lowered further until the inert plastic growth surface was in focus (Figure 3). The difference in fine adjustment settings was compared with a calibration curve, and the thickness was determined. The reported biofilm thickness was the mean of 4 or 5 measurements along the slide from top to bottom.

After the last biofilm measurement in an experiment, the removable slide was dried (60°C, 1 hour) and weighed. The slide was then cleaned, dried, and weighed again. The difference in the two measurements was the dry film mass. The volumetric film density, which has units of dry mass per unit wet volume, could then be calculated. The 60°C/1-hour drying conditions were used to prevent warping of the acrylic plastic slide.

Glucose concentration was determined enzymatically and the calibration curves consistently exhibited linear behavior in the desired concentration range.

Suspended solids were determined by filtering 150

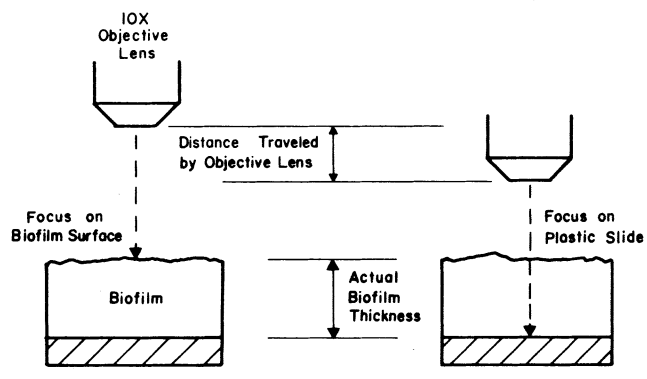

Figure 3—Representation of biofilm thickness measurement.

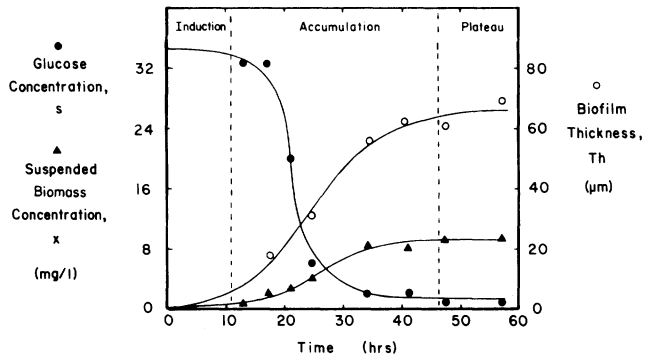

Figure 4—Typical experimental progression.

cm^3 of the reactor effluent through a micropore membrane (average pore size = 0.45 μm). The filters were dried at 60°C for a minimum of 3 hours and then weighed.

The experiments were initiated by inoculating with a mixed population of microorganisms and operating the reactor in a batch mode (as opposed to continuous flow) until some surface colonization occurred (8 hours). This technique minimized the induction period (Figure 4), which could last for weeks under some of the conditions tested.

A standard microbial inoculum was prepared to minimize the effects of population distribution differences in the experiments. Twenty litres of mixed liquor from a domestic wastewater treatment plant (Bellaire, Tex.) was settled and the concentrated sludge mixed with glycerol to approximately 25% glycerol. Portions (10 cm^3) of the resulting suspension were transferred to glass ampules that were "quick-frozen" in liquid nitrogen and then stored at −20°C. Growth rate tests of the standard inocula were conducted periodically and indicated no significant changes over a period of 1 year.

Further details concerning methods and apparatus may be found elsewhere.[9]

RESULTS

The overall process of biofilm development may be conveniently divided into three phases:

- Induction,
- Accumulation, and
- Plateau.

These phases are indicated in Figure 4.

The *induction* phase is characterized by the development of a primary layer of biofilm on an initially "clean" surface. Organic adsorption, followed by the transport and attachment of microorganisms to the surface, are significant rate processes during the induction period.

The induction period is followed by the accumulation phase, which may be characterized by two substages—a logarithmic increase followed by a nearly constant accumulation rate. The logarithmic portion begins in the latter stages of the induction period and continues until a "critical" film thickness is attained. At the critical thickness, glucose removal reaches a steady-state value, and is not affected by additional film accumulation. A period of near-constant accumulation is then observed; this period is terminated when the shearing of the biofilm prevents further accumulation.

The last period is the *plateau* phase in which new biofilm production equals the biofilm being sheared from the surface by the fluid. Hence, during the plateau phase, biofilm thickness remains essentially constant.

The suspended biomass concentration increases with biofilm thickness. In the biofilm reactor used for this study, the influent suspended biomass concentration was zero. Furthermore, the reactor was operated at a hydraulic retention time of 10 minutes so that biomass production resulting from growth processes would be limited to the attached biomass. Hence, the increase in suspended solids with time may be directly attributed to the process of biofilm detachment.

Mass conservation equations. A material balance approach was used to account for the removal of substrate from the bulk fluid, the accumulation of attached biomass, and the production of suspended biomass.

A mass balance across the reactor on the limiting nutrient, glucose, is as follows:

$$V\frac{ds}{dt} = F(s_i - s) - R_g A - R'_g V \qquad (1)$$

net rate of glucose accumulation = *net rate of glucose input by flow* − *rate of glucose removal for biomass production*

where

V = reactor volume (L^3),
s = glucose reactor concentration (ML^{-3}),
t = time (t),
F = volumetric flow rate of the reactor feed (L^3t^{-1}),
s_i = influent glucose concentration (ML^{-3}),
R_g = attached biomass glucose removal rate per unit wetted surface area ($ML^{-2}t^{-1}$),
A = reactor wetted surface (L^2), and
R'_g = suspended biomass glucose removal rate per unit reactor volume ($ML^{-3}t^{-1}$).

L, M, and t represent length, mass, and time units, respectively

The removal of substrate by suspended biomass is assumed negligible in comparison to substrate consumption by attached biomass because of the relatively small

quantity of suspended biomass in the reactor. Neglecting the substrate removal term by suspended biomass, Equation 1 may be rewritten as

$$V\frac{ds}{dt} = F(s_i - s) - R_g A \tag{2}$$

An inventory of the total biomass in the system is as follows:

$$\underset{\text{total biomass}}{M_T} = \underset{\text{attached biomass}}{A\rho Th} + \underset{\text{suspended biomass}}{Vx} \tag{3}$$

where

M_T = total reactor biomass (M),
ρ = biofilm volumetric density (ML^{-3}),
Th = biofilm thickness (L), and
x = suspended biomass reactor concentration (ML^{-3}).

For constant V, A, and ρ, the change in total biomass with time is

$$\frac{dM_T}{dt} = A\rho\frac{dTh}{dt} + V\frac{dx}{dt} \tag{4}$$

where $A\rho(dTh/dt)$ and $V(dx/dt)$ represent the net accumulation of attached and suspended biomass. Although biofilm density is assumed constant during a given experiment, it does vary between experiments.

The accumulation of attached biomass will be considered the net result of two processes:

1. Biomass production resulting from growth and exopolymer production, and
2. Biofilm detachment by fluid shear forces.

Representing the biomass production rate as the product of the glucose removal rate and the biomass yield coefficient, the net accumulation of attached biomass may be written as follows:

$$\underset{\substack{\text{net rate of attached}\\ \text{biomass accumulation}}}{A\rho\frac{dTh}{dt}} = \underset{\substack{\text{rate of attached}\\ \text{biomass production}}}{R_g YA} - \underset{\substack{\text{rate of biofilm}\\ \text{detachment}}}{R_d A} \tag{5}$$

where

Y = biomass yield coefficient (MM^{-1}), and
R_d = biofilm detachment rate per unit wetted surface area ($ML^{-2}t^{-1}$).

Equation 5 may be rearranged to obtain an expression for Y

$$Y = \frac{A\rho\dfrac{dTh}{dt} + R_d A}{R_g A} \tag{6}$$

A mass balance across the reactor for suspended biomass is as follows:

$$\underset{\substack{\text{net rate of}\\ \text{suspended biomass}\\ \text{accumulation}}}{V\frac{dx}{dt}} = \underset{\substack{\text{net rate of}\\ \text{input by flow}}}{F(x_i - x)} + \underset{\substack{\text{rate of biofilm}\\ \text{detachment}}}{R_d A} + \underset{\substack{\text{rate of growth}\\ \text{of suspended}\\ \text{biomass}}}{R'_g Y' V} \tag{7}$$

where

x_i = influent suspended biomass concentration (ML^{-3}), and
Y' = suspended biomass yield coefficient (MM^{-1}).

Because the influent suspended biomass concentration was zero and the reactor hydraulic retention time was 10 minutes, the production of suspended biomass resulting from dispersed growth is assumed negligible. Hence, Equation 7 may be rewritten as follows:

$$V\frac{dx}{dt} = -Fx + R_d A \tag{8}$$

The process rates for glucose removal and biofilm detachment, R_g and R_d, and the biomass stoichiometric yield coefficient, Y, are the quantities of concern because they determine the rate and extent of biofilm accumulation. To facilitate analysis of these quantities, glucose removal, biofilm thickness, and suspended biomass experimental data are time-smoothed using the following logistics equation:

$$Z = \frac{Z_0 e^{k't}}{1 - \left(\dfrac{Z_0}{Z_m}\right)(1 - e^{k't})} \tag{9}$$

where

$Z = (s_i - s)$, Th or x;
Z_0 = Z at time $t = 0$;
Z_m = maximum value attained; and
k' = rate constant.

The rate of change of Z may be described by the following:

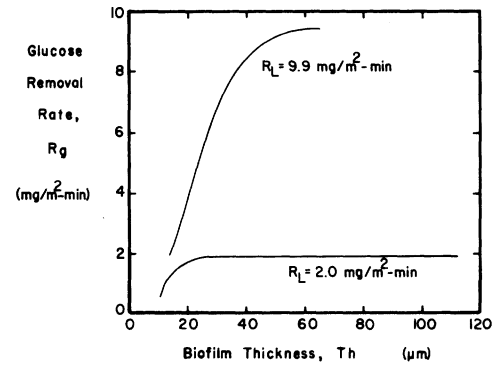

Figure 5—Change in glucose removal rate with biofilm thickness.

$$\frac{dZ}{dt} = k'Z - \frac{k'Z^2}{Z_m} \tag{10}$$

Glucose removal rate. The variation in glucose removal rate, R_g, with biofilm thickness is shown in Figure 5 for two experiments at different glucose loading rates. The glucose loading rate is defined as follows:

$$R_L = \frac{Fs_i}{A} \tag{11}$$

where

R_L = glucose loading rate ($ML^{-2}t^{-1}$).

The removal rate increases in proportion to biofilm thickness up to a critical thickness beyond which removal rate remains constant. This critical thickness will be termed the "active" thickness, Th_A. Th_A is observed to increase with the glucose concentration in the reactor (Figure 6).

R_g increases with the rotational speed of the inner cylinder. Figure 7 indicates the increase is substantial for speeds less than 170 rev/min (93.5 cm/s). The data in Figure 7 were obtained by developing a mature biofilm at 200 rev/min, reducing the rotational speed to one of the test speeds, and determining the glucose removal after a 1-hour transition period.

Biomass production rate. The production of biomass in the reactor was limited to growth processes occurring on the reactor surfaces. The rate of biomass production

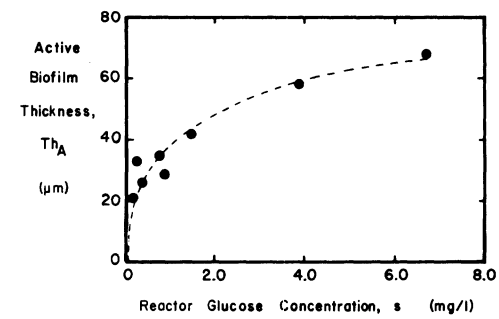

Figure 6—Relation betweeen active biofilm thickness and reactor glucose concentration.

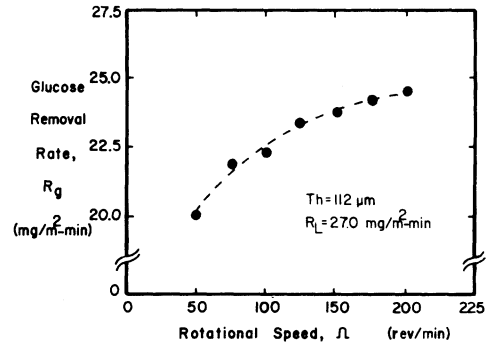

Figure 7—Variation in glucose removal rate with rotational speed.

is discussed by defining a specific production rate, r_p, as follows:

$$r_p = \frac{1}{M_T}\frac{dM_T}{dt} \tag{12}$$

where

r_p = specific production rate (t^{-1}), and
M_T = total biomass in reactor (M).

Substituting for dM_T/dt from Equations 4, 5, and 8

$$r_p = \frac{R_g YA - Fx}{M_T} \tag{13}$$

The relation between r_p and reactor glucose concentration is shown in Figure 8 for two experiments with different glucose loading rates. Figure 8 indicates that r_p is a hyperbolic function of s and, hence, r_p may be mathematically related to s by an equation of the following form:

$$r_p = \frac{r_{pmax}s}{K_p + s} \tag{14}$$

where

r_{pmax} = maximum specific production rate (t^{-1}), and
K_p = saturation constant (ML^{-3}).

Biofilm detachment rate. The biofilm detachment rate, R_d, increases with the mass of attached biofilm, as shown in Figure 9. Figure 10 indicates that R_d increases with rotational speed for a given mass of biofilm.

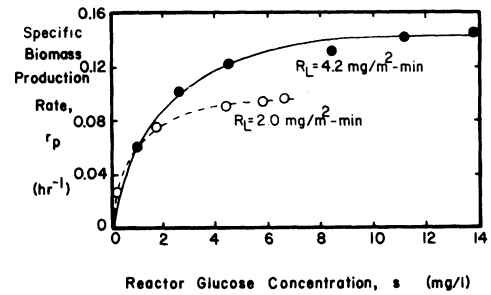

Figure 8—Relation between specific biomass production rate and reactor glucose concentration.

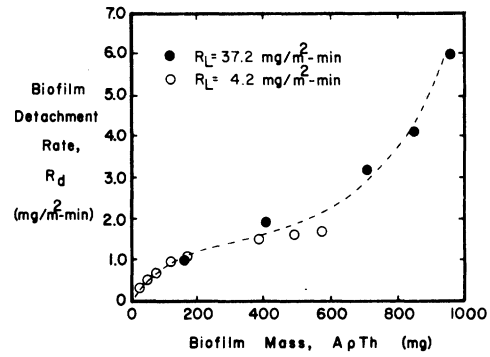

Figure 9—Change in biofilm detachment rate with biofilm mass.

Net biofilm accumulation. The net result of the processes of biomass production and biofilm detachment is the accumulation of attached biofilm. The net biofilm accumulation rate per unit wetted surface area, $\rho(dTh/dt)$, increases with time to a maximum and then decreases to zero as the biofilm thickness approaches a plateau value (Figure 11). The rate illustrated in Figure 11 corresponds to the biofilm thickness data in Figure 4.

The maximum net biofilm accumulation rate, $\rho(dTh/dt_{max})$, increases with glucose loading rate as shown in Figure 12. Figure 13 illustrates the variation in $\rho(dTh/dt_{max})$ with rotational speed for a given glucose loading rate.

The plateau mass of attached biofilm per wetted surface area, ρTh_p, is indicative of the extent of biofilm accumulation. ρTh_p increases with glucose loading rate as shown in Figure 14. Although the mass of biofilm increases, the plateau thickness, Th_p, decreases (Figure 14). Figure 15 indicates the variation in ρTh_p with rotational speed for a given glucose loading rate.

Biomass yield coefficient. The biomass yield coefficient, Y, varies with experimental run time. Figure 16 indicates that changes in Y during a given experiment vary with glucose loading rate.

Biofilm density and morphology. Biofilm *density* (ρ) increases with glucose loading rate as shown in Figure 17. Biofilm *morphology* was observed microscopically

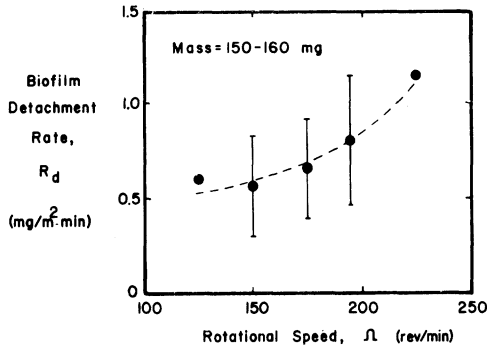

Figure 10—Change in biofilm detachment rate with rotational speed.

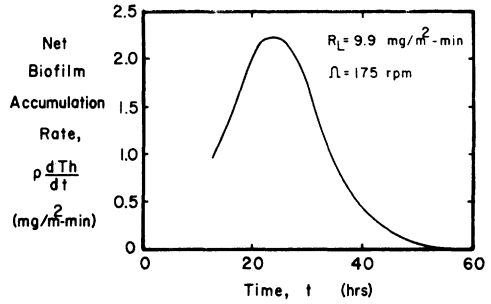

Figure 11—Variation in the net biofilm accumulation rate with time.

during biofilm thickness measurements. Largely filamentous biofilms were observed in experiments with low glucose loading rates. With increasing glucose loading, the biofilm structure shifted to a nonfilamentous matrix predominated by dense patches of microbial colonies.

The observed trends in biofilm density and morphology suggest that the density of the biofilm decreases with increasing filamentous structure.

Frictional resistance. Frictional resistance in the annular reactor may be represented by a dimensionless friction factor defined by the following equation:[10]

$$f_a = \frac{T_q}{0.5\pi\rho_w V_i^2 R_i^2 H} \qquad (15)$$

where

T_q = torque on inner cylinder (ML^2t^{-2}),
ρ_w = density of water (ML^{-3}),
V_i = peripheral velocity of inner cylinder (Lt^{-1}),
R_i = radius of inner cylinder (L), and
H = height of inner cylinder (L).

The relation between f_a and biofilm thickness as a function of biofilm density is shown in Figure 18. Once a certain minimum thickness is reached, f_a increases linearly with Th.

DISCUSSION

Glucose removal rate. The utilization of substrate by a microbial film is a heterogeneous process because two

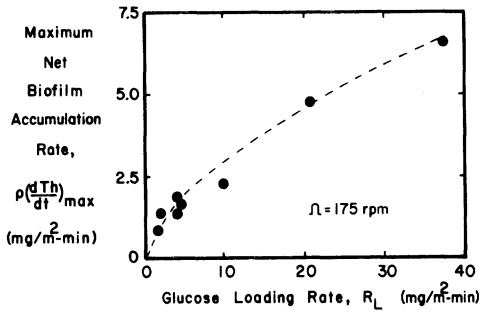

Figure 12—Change in the maximum net biofilm accumulation rate with glucose loading rate.

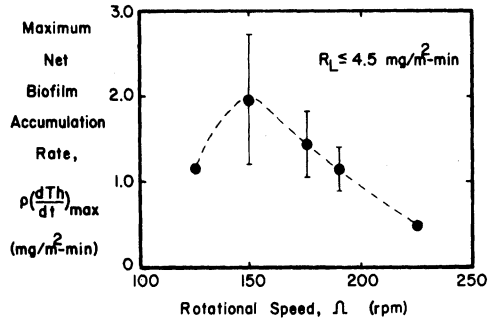

Figure 13—Variation in maximum net biofilm accumulation rate with rotational speed.

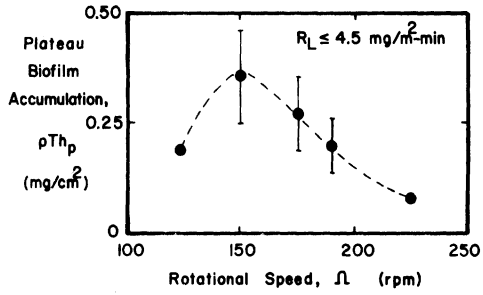

Figure 15—Variation in plateau biofilm accumulation with rotational speed.

phases (solid and liquid) are required. The kinetics of a heterogeneous process demand consideration of the reaction and the diffusion of reactants in each phase because limitations in reactant transport can significantly affect the rate of the overall process.

For the substrate-biofilm reaction, the following diffusion and reaction processes are of concern:

1. Substrate (electron donor plus nutrients) and oxygen (electron acceptor) diffusion from the bulk of the liquid to the fluid-biofilm interface,
2. Substrate and oxygen diffusion within the biofilm,
3. Biochemical reaction (substrate consumption) within the film, and
4. Out-diffusion of metabolic products from within the biofilm to the bulk solution.

Liquid phase diffusion. The transport of glucose from the bulk liquid to the fluid-biofilm interface may be represented by the following expression:

$$N = k_L(s - s_s) \qquad (16)$$

where

N = glucose flux to the surface ($ML^{-2}t^{-1}$),
k_L = mass transfer coefficient (Lt^{-1}),
s = glucose concentration in the bulk solution (ML^{-3}), and
s_s = glucose concentration at the film surface (ML^{-3}).

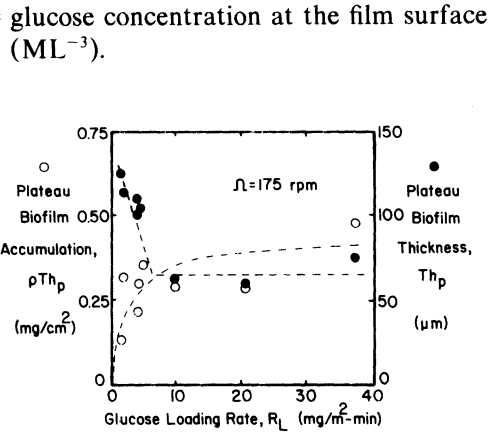

Figure 14—Change in plateau biofilm accumulation and plateau biofilm thickness with glucose loading rate.

Under steady-state conditions, the amount of glucose transported to the biofilm surface must equal the amount of glucose consumed by the biofilm. This equality may be written as follows:

$$R_g A = NA \qquad (17)$$

Lamotta[11] investigated liquid phase diffusion and identified two limiting regimes, depending on the magnitude of the mass transfer coefficient. When k_L is large, the microorganisms in the biofilm receive a maximum amount of glucose, and the rate of the overall process (R_g) is determined by the kinetics of the internal diffusion-reaction process. Under these conditions, the kinetics of the internal diffusion-reaction process may be measured, because diffusional resistance resulting from the liquid phase is insignificant.

However, when the mass transfer coefficient is small, substrate concentration at the biofilm surface is essentially zero. Under these conditions, liquid phase diffusional resistance is significant, and the rate of the overall process (R_g) is determined by the rate of glucose transport to the biofilm surface.

The transition from significant to negligible liquid phase diffusional resistance may be achieved by increasing fluid velocity at the biofilm surface.[7,11,12]

The data in Figure 7 suggest that liquid phase resistance in the annular reactor used in this study is negligible for rotational speeds greater than 170 rev/min (93.5 cm/s), because the glucose removal rate is relatively insensitive to rotational speed in this region. La-

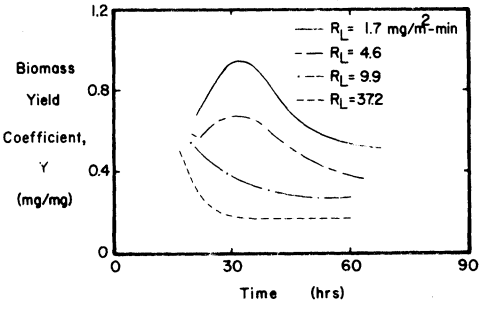

Figure 16—Variation in biomass yield coefficient with time.

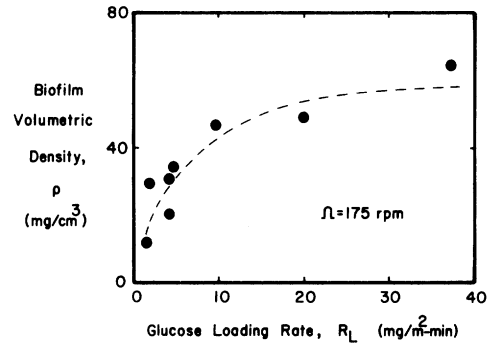

Figure 17—Relation between biofilm volumetric density and glucose loading rate.

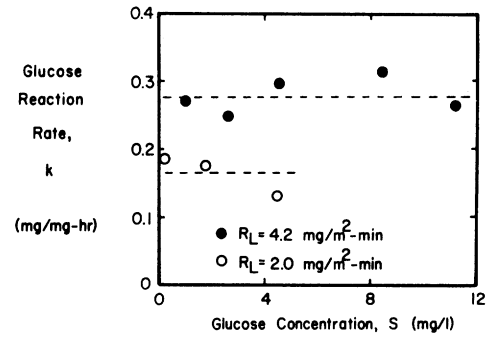

Figure 19—Glucose reaction rate as a function of reactor glucose concentration (rotational speed = 175 rev/min).

motta,[11] using an annular reactor with a stationary inner cylinder and a rotating outer cylinder, reports liquid phase resistance in his system was minimized once the rotational speed exceeded 96 rev/min (80 cm/s).

The results reported in this and other studies[7,11-14] suggest that unless liquid phase diffusional resistances are minimized, the substrate removal efficiency of biological film systems may be limited by the transport of reactants from the bulk liquid to the fluid-biofilm interface.

Equations for internal diffusion and reaction. Equations describing internal substrate diffusion and reaction within a biofilm are developed and presented elsewhere.[15,16] Assuming the rate of reaction is limited only by the availability of glucose, the results depend on whether there is complete or incomplete glucose penetration within the biofilm.

For the case of a *fully penetrated biofilm*

$$R_g = k\rho Th \tag{18}$$

and for the case of a *partially penetrated biofilm*

$$R_g = k\rho Th_a \tag{19}$$

where

k = zero-order reaction rate coefficient ($Mt^{-1}M^{-1}$), and

Th_a = active thickness—that is, the thickness of biofilm active in consuming glucose (L).

Equation 19 indicates that when there is incomplete penetration, the reaction rate depends on the depth of penetration and is independent of the total biofilm thickness.

Glucose reaction rate. For the condition of negligible liquid phase diffusional resistance, the equations obtained for R_g may be combined with Equation 2 to yield the following:

fully penetrated film

$$V\frac{ds}{dt} = F(s_i - s) - k\rho ATh \tag{20}$$

partially penetrated film

$$V\frac{ds}{dt} = F(s_i - s) - k\rho ATh_a \tag{21}$$

These equations may be used to determine the reaction rate k from either known or measured quantities.

Values of k determined from Equations 20 and 21 for two experiments with different glucose loading rates are shown in Figure 19. The rate shows little dependence on the bulk glucose concentration, particularly at the high glucose loading rate. This suggests that the reaction may be adequately described by zero-order

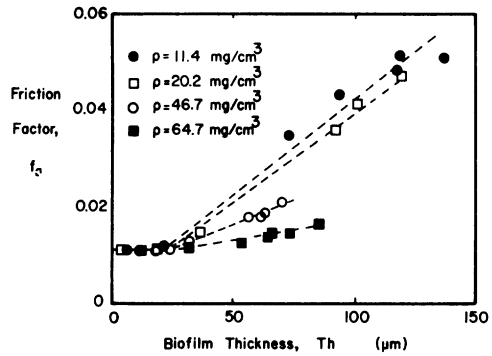

Figure 18—Relation between friction factor and biofilm thickness as a function of biofilm density.

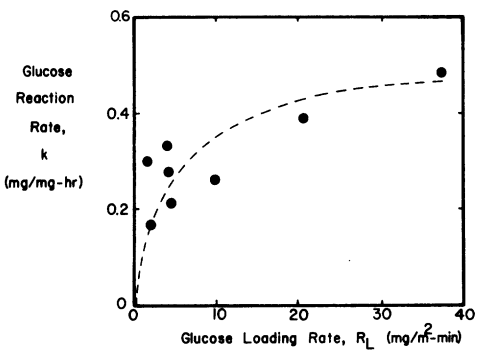

Figure 20—Variation in glucose reaction rate with glucose loading rate (rotational speed = 175 rev/min).

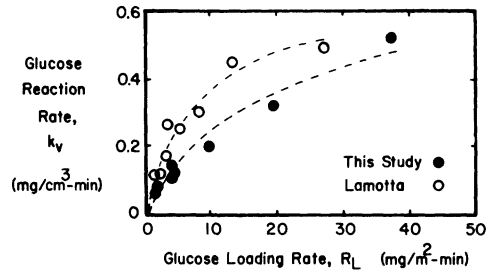

Figure 21—Comparison of glucose reaction rate data from Lamotta[17] with this study.

kinetics. Deviations from zero order at the low glucose loading rate are attributed to an incomplete coverage of biofilm in the reactor during the early stages of the experiment. Zero-order reaction kinetics have also been reported by other investigators dealing with biofilm systems.[15,17,18]

The reaction rate k increases with glucose loading rate as shown in Figure 20. This behavior is also reported by Zelver[18] in a tubular reactor system and by Lamotta[17] in an annular reactor. Lamotta did not determine biofilm density in his study; hence, his reaction rate data are reported per unit biofilm volume (mg/cm^3 · min). Figure 21 is a comparison of Lamotta's data with reaction rate values obtained in this study, which is corrected for Lamotta's units. The rates from these two studies increase with glucose loading rate in a very similar manner.

Lamotta, based on his own work and on results obtained by Gaudy *et al.*,[19] concludes that the concentration of substrate present in the early stages of film development determines the number of cell permeation sites and hence the substrate uptake rate. Lamotta used this reasoning to explain the observed relation between glucose loading rate and k. Although the data suggest some consistency as a function of loading rate, there is no assurance that substrate loading can adequately describe the phenomena.[15]

Results obtained in this study suggest that the observed relation between k and glucose loading rate may be due to changes in biofilm density, because biofilm density also varies with glucose loading.

Table 4—Biomass yield coefficients.

Reference	Glucose loading rate (mg/m^2 · min)	Biomass yield $\left(\frac{\text{mg biomass}}{\text{mg glucose}}\right)$
Kornegay[7]	60–200[a]	0.21–0.32[b]
Lamotta[17]	1.5–133.4	5.8×10^{-3}[c]
Zelver[18]	25.7	0.13–0.33[d]

[a] Estimated from glucose removal rates.
[b] Range of 10 steady-state values.
[c] cm^3 of biofilm/mg glucose.
[d] Variation during 1 experiment.

Oxygen limitations. The glucose-biofilm reaction also may be limited by the availability of oxygen, the exogenous electron acceptor.[20–23] When insufficient oxygen is available for complete oxidation of the glucose to biomass and CO_2, soluble organic intermediates are formed that can diffuse out of the film and accumulate in the bulk liquid.[24,25]

The possibility of an oxygen limitation in this study is discussed elsewhere.[9] The results suggest that the glucose-biofilm reaction may have been limited by the availability of oxygen once the glucose removal rate exceeded 4.0 mg/m^2 · min.

Biomass yield coefficient. The biomass yield coefficient, Y, is defined as the observed ratio between biomass production rate and glucose removal rate. As Figure 16 indicates, the magnitude of Y may vary significantly during a typical experiment.

Previous investigators[7,17,18] have also measured biomass yields in biofilm systems utilizing glucose as the sole carbon source (Table 4). Zelver[18] observed a variation in Y; however, the reported data do not follow any consistent trends. A constant biofilm yield is reported by Lamotta[17] during the logarithmic accumulation phase and by Kornegay and Andrews[7] during steady-state conditions.

The variations in yield that were observed in this study are attributed to one or a combination of the following processes, which have been implicated in previous biofilm studies.[15,23–28]

- Exopolymer production,
- Oxygen limitations, and
- Biomass decay.

Exopolymer production. Biofilms contain a high proportion of exopolymer material.[26–28] The exopolymer is postulated to play an important role in maintaining the structural integrity of the biofilm matrix. The relative exopolymer content of the biofilm is reported to change with biofilm development.[28] Because biofilm production is the combined effect of cellular reproduction and exopolymer production, variations in exopolymer production affect the magnitude of Y.

Table 5—Maximum specific production rate and saturation constant data.

Glucose loading rate, R_L (mg/m^2 · min)	Maximum specific production rate, r_p (h^{-1})	Saturation constant, K_p (mg/l)
2.0	0.11	0.6
4.1	0.14	0.9
4.2	0.17	1.9
4.6	0.10	0.5
9.9	0.20	10.3
20.6	0.35	30.0
37.2	0.52	69.8
37.6–376.0[7]	0.28	121.0
1.5–27.0[17]	0.19	7.8

Williams and Wimpenny[29] and Mian *et al.*[30] report exopolysaccharide yields that approach 0.8 (mg exopolysaccharide/mg glucose) in dispersed biomass systems where glucose was used as the sole carbon source. This value (0.8) suggests that the relatively high yields observed in this study may be indicative of periods of substantial exopolysaccharide production.

Oxygen limitations. Oxygen limitations within the biofilm frequently result in the formation of soluble organic intermediates.[24,25] The formation of these intermediates may be an important process in this study, particularly at the high glucose loading rates.

Metabolic intermediate formation would cause a decrease in Y because less carbon and energy for biomass production could be derived per glucose molecule. Oxygen limitations and intermediate product formation may contribute to the observed decrease in Y with increasing glucose loading rate, especially in the latter stages of an experiment.

Biomass decay. Biomass decay could also be responsible for causing variations in Y. Once the active biofilm thickness is reached and glucose is depleted in the lower layers of the biofilm, endogenous metabolism may be significant. This could account for the decrease in Y that is observed in the latter stages of biofilm development.

Specific biomass production rate. The specific biomass production rate is described by an equation of the same form proposed by Monod[31] to describe dispersed microbial growth. Specific rate constants obtained from this study along with constants reported by Kornegay and Andrews[7] and Lamotta[17] are given in Table 5.

Saturation constant data from biofilm studies must be used with caution because of the effect of diffusional resistances within the biofilm.[15] Saturation constants for dispersed organisms utilizing glucose are reported to be in the range of 0.1 to 5.0 mg/l, depending on the particular organism.[32] Values obtained exceeding this range suggest the presence of diffusional resistances. Hence, the high saturation values reported in Table 5 may correspond to experiments where either glucose or oxygen diffusional resistances were significant.

Biofilm detachment rate. Biofilm detachment is reported to depend on the fluid shear stress at the fluid-biofilm interface.[18,33,34] Exterior portions of the attached biofilm are assumed to be continuously sheared into the fluid. The rate of shear removal is suggested to increase in proportion to the interfacial fluid shear stress. The results in this study support the assertion that biofilm detachment rate increases with increasing shear stress because the latter increases with both biofilm mass and rotational speed.

The data in Figure 9 indicate that the detachment rate approaches an infinitely large value at high biofilm mass. This behavior agrees with the results reported by Zelver,[9] which indicate fluid shear stress can limit the maximum quantity of attached biofilm in a turbulent flow regime.

Net biofilm accumulation. Biofilm accumulation is the net result of glucose removal, attached biomass production, and biofilm detachment. The rate and extent of biofilm accumulation are quantities of concern when dealing with biofilm systems.

The maximum net biofilm accumulation rate, $\rho(dTH/dt_{max})$, increases with glucose loading (Figure 12) because of an increased glucose concentration in the reactor. The relation is not linear, and the data suggest $\rho(dTh/dt_{max})$ will reach a maximum asymptotic value at higher glucose loading rates.

The relation between $\rho(dTh/dt_{max})$ and rotational speed is shown in Figure 13. The increase in $\rho(dTh/dt_{max})$ is attributed to a decrease in liquid phase resistance and hence a higher concentration of glucose at the fluid-biofilm interface. However, as the rotational speed is increased further, the effects of biofilm detachment become more important, and thus a decrease in $\rho(dTh/dt_{max})$ is observed.

The plateau value for attached biofilm mass, ρTh_p, increases with glucose loading (Figure 14); however, the rate of increase diminishes significantly once the glucose loading rate approaches 10 mg/m^2·min. This behavior may be caused by a limitation in oxygen at the higher glucose loading rates.

The plateau biofilm thickness, Th_p, decreases with glucose loading (Figure 14) although ρTh_p increases. This condition is the result of an increase in biofilm density with glucose loading rate (Figure 17). Zelver,[18] using a tubular reactor system, also observed an increase in biofilm density with glucose loading. However, in Zelver's experiments, both plateau biofilm thickness and mass increased with glucose loading.

ρTh_p varies with rotational speed, as illustrated in Figure 15. This figure also depicts the general form of the relation between Th_p and rotational speed in the indicated range of glucose loading rate. This trend is attributed to the same interplay between decreased liquid phase resistance and increased biofilm detachment that is discussed above for the maximum net biofilm accumulation rate.

Biofilm density and morphology. The results obtained concerning biofilm density and morphology suggest that different microbial species are preferentially selected for in the biofilm depending on the level of influent glucose. At the low glucose loading rates, filamentous organisms with a high surface-area-to-volume ratio dominated. These organisms would have a physiological advantage over other morphological forms because they could protrude into the bulk fluid and "see" more glucose.

Photomicrographs of the filamentous biofilms observed in this study closely resemble photographs of attached *Sphaerotilus* growth presented by Dias *et al.*[35]

Furthermore, Dias *et al.* report that low influent glucose favored greater numbers of filamentous *Sphaerotilus* in the mixed population slimes developed.

Frictional resistance. Zelver[18] extensively investigated the increase in frictional resistance resulting from biofilm development in a tubular reactor system with the following results:

1. Frictional resistance resulting from biofilm development causes an increase in pressure drop and power requirements for pumping in experiments where flow rate is maintained constant. Conversely, flow capacity is reduced if pressure drop is held constant.
2. Frictional resistance resulting from biofilm development shows a similar dependence on Reynolds number as frictional resistance, which is due to commercially rough pipe surfaces.
3. Frictional resistance is dependent on biofilm thickness.
4. Frictional resistance does not increase above the hydraulically smooth pipe value until a critical biofilm thickness, approximately equal to the thickness of the viscous sublayer, is attained. The critical thickness apparently corresponds to the stage of biofilm accumulation at which surface irregularities protrude through the viscous sublayer. Preceding this stage, the roughness peaks are smaller than the viscous sublayer; and the friction factor does not increase (the tube is hydraulically smooth).

Results obtained in this study that relate frictional resistance to surface roughness agree with the results reported by Zelver and are discussed elsewhere.[9]

Zelver[18] and Picologlou *et al.*[36] indicate that although the increase in frictional resistance may be adequately described by formulae suitable for rigid rough surfaces, the conclusion should not be drawn that the biofilm presents a rigid surface to the flow. To the contrary, it is suggested that the mechanism of energy dissipation is related to the viscoelastic properties and the filamentous structure of the biofilm.

The results from this study also indicate that biofilm structure contributes significantly to the increase in frictional resistance. In experiments where filamentous biofilms developed, strands of attached biofilm were observed to flutter with a frequency that was a function of the reactor fluid velocity. This suggests that filamentous strands of biofilm may play a substantial role in dissipating energy and thus in causing the observed increase in frictional resistance.

SUMMARY

This research has provided insight into the processes associated with biofilm accumulation. Specifically:

1. Biofilm accumulation is the net result of substrate removal, biofilm production resulting from metabolic growth, and biofilm detachment caused by fluid shear.
2. Glucose removal is directly proportional to biofilm thickness up to an active thickness that corresponds to the depth of glucose penetration into the biofilm.
3. The depth of glucose penetration increases with increasing reactor glucose concentration.
4. Glucose removal is limited by the transfer of glucose from the bulk liquid to the fluid-biofilm interface at low fluid velocities.
5. The rate and extent of biofilm accumulation increase with glucose loading rate.
6. The rate and extent of biofilm accumulation increase with fluid velocity at low velocities and decrease with increasing fluid velocity at high velocities.
7. Biofilm detachment increases with fluid velocity and the mass of attached biofilm.
8. Biofilm density increases with glucose loading rate.
9. Biofilm density and morphology are related. Low density biofilms exhibit a filamentous structure. High density biofilms exhibit a nonfilamentous structure characterized by dense patches of microbial colonies.
10. Biofilm accumulation increases fluid frictional resistance. Once a critical biofilm thickness is reached, frictional resistance increases in proportion to biofilm thickness. For a given biofilm thickness, frictional resistance increases with filamentous structure.

ACKNOWLEDGMENTS

Credits. This research study was partially funded by the Electric Power Research Institute (RP-902), the National Science Foundation (ENG 74-11957), Calgon Corporation, and the Office of Naval Research (N00014-80-C-0475). B. F. Picologlou and L. V. McIntire made significant contributions to the experimental program, and Willi Gujer contributed valuable comments concerning data analysis. The work was conducted in the Department of Environmental Science and Engineering, Rice University, Houston, Tex., by M. G. Trulear under the direction of W. G. Characklis. The manuscript was prepared at Montana State University, Bozeman, Mont. The paper was originally presented at the 53rd Annual Conference of the Water Pollution Control Federation, Las Vegas, Nev., Sept. 28–Oct. 3, 1980.

Authors. Currently, Michael G. Trulear is senior engineer, Nalco Chemical Co., and William G. Characklis is a professor, Department of Civil Engineering, Montana State University, Bozeman. Correspondence should be addressed to Michael G. Trulear, Nalco Chemical Co., 1801 Diehl Rd., Naperville, IL 60566.

APPENDIX

Symbol	Definition	Dimensions
A	Reactor wetted surface area	(L^2)
F	Volumetric flow rate	(L^3t^{-1})

Symbol	Definition	Dimensions
f_a	Friction factor	(dimensionless)
H	Height of the inner cylinder	(L)
k	Glucose reaction rate	$(MM^{-1}t^{-1})$
k'	Time-smoothing constant	(t^{-1})
k_L	Mass transfer coefficient	(Lt^{-1})
k_p	Production rate saturation constant	(ML^{-3})
k_v	Glucose reaction rate per biofilm volume	$(ML^{-3}t^{-1})$
M_T	Total reactor biomass	(M)
N	Glucose flux	$(ML^{-2}t^{-1})$
R_d	Biofilm detachment rate per unit wetted surface area	$(ML^{-2}t^{-1})$
R_g	Attached biomass glucose removal rate per unit wetted surface area	$(ML^{-2}t^{-1})$
R'_g	Suspended biomass glucose removal rate per unit reactor volume	$(ML^{-3}t^{-1})$
R_i	Radius of inner cylinder	(L)
R_L	Glucose loading rate	$(ML^{-2}t^{-1})$
r_p	Specific biomass production rate	(t^{-1})
s	Reactor glucose concentration	(ML^{-3})
s_i	Influent glucose concentration	(ML^{-3})
s_s	Glucose concentration at the biofilm surface	(ML^{-3})
t	Time	(t)
Th	Biofilm thickness	(L)
Th_a	Active biofilm thickness	(L)
Th_p	Plateau biofilm thickness	(L)
T_q	Torque on inner cylinder	(ML^2t^{-2})
V	Reactor volume	(L^3)
V_i	Peripheral velocity of inner cylinder	(Lt^{-1})
x	Suspended biomass concentration	(ML^{-3})
Y	Biomass yield coefficient	(MM^{-1})
Y'	Suspended biomass yield coefficient	(MM^{-1})
ρ	Biofilm density	(ML^{-3})
ρ_w	Density of water	(ML^{-3})

L, M, and t represent length, mass, and time units, respectively

REFERENCES

1. Baier, R. E., "Applied Chemistry at Protein Interfaces." *Adv. Chem. Ser., Am. Chem. Soc.*, **145,** 1 (1973).
2. Baier, R. E., "Influence of the Initial Surface Condition of Materials on Bioadhesion." *Proc. 3rd Int. Congr. Mar. Corros. Biofouling*, Gaithersburg, Md. (1972).
3. Baier, R. E., and Depalma, V. A., "Microfouling of Metallic and Coated Metallic Flow Surfaces in Model Heat Exchanger Cells." *Calspan Corp. Rep.*, Buffalo, N. Y. (1977).
4. Baier, R. E., *et al.*, "Adhesion: Mechanisms that Assist or Impede It." *Science,* **162,** 1360 (1968).
5. Marshall, K. C., *et al.*, "Mechanisms of the Initial Events in the Sorption of Marine Bacteria to Surfaces." *J. Gen. Microbiol.*, **68,** 337 (1971).
6. Zobell, C. E., "The Effects of Solid Surfaces Upon Bacterial Activity." *J. Bacteriol.*, **46,** 39 (1943).
7. Kornegay, B. H., and Andrews, J. F., "Characteristics and Kinetics of Biological Film Reactors." FWPCA Final Rep., Res. Grant WP-01181, Dept. Environ. Systems Eng., Clemson Univ., Clemson S. C. (1967).
8. Sanders, W. M., III, "The Relationship Between the Oxygen Utilization of Heterotrophic Slime Organisms and the Wetted Perimeter." Ph. D. dissertation, Johns Hopkins Univ., Baltimore, Md. (1964).
9. Trulear, M. G., "Dynamics of Biofilm Processes in an Annular Reactor." M.S. thesis, Rice Univ., Houston, Tex. (1980).
10. Schlichting, H., "Boundary Layer Theory." McGraw-Hill Book Co., New York, N. Y. (1968).
11. Lamotta, E. J., "External Mass Transfer in a Biological Film Reactor." *Biotechnol. Bioeng.*, **18,** 1359 (1976).
12. Maier, W. J., *et al.*, "Simulation of the Trickling Filter Process." *J. Sanit. Eng. Div. Proc. Am. Soc. Civ. Eng.*, **93,** 91 (1967).
13. Gulevich, W., "The Role of Diffusion in Biological Waste Treatment." Ph. D. dissertation, Johns Hopkins Univ., Baltimore, Md. (1967).
14. Gulevich, W., *et al.*, "Role of Diffusion in Biological Waste Treatment." *Environ. Sci. Technol.*, **2,** 113 (1968).
15. Harremoes, P., "Biofilm Kinetics." In "Water Pollution Microbiology." R. Mitchell (Ed.), John Wiley and Sons, New York, N. Y., Vol. 2, 71 (1978).
16. Lamotta, E. J., "Internal Diffusion and Reaction in Biological Films." *Environ. Sci. Technol.*, **10,** 765 (1976).
17. Lamotta, E. J., "Kinetics of Growth and Substrate Uptake in a Biological Film System." *Appl. Environ. Microbiol.*, **31,** 286 (1976).
18. Zelver, N., "Biofilm Development and Associated Energy Losses in Water Conduits." M.S. thesis, Rice Univ., Houston, Tex. (1979).
19. Gaudy, A. F., *et al.*, "Control of Growth Rate by Initial Substrate Concentration." *Appl. Microbiol.*, **22,** 1041 (1971).
20. Bungay, H. R., III, *et al.*, "Microprobe Techniques for Determining Diffusivities and Respiration Rates in Microbial Slime Systems." *Biotechnol. Bioeng.*, **6,** 765 (1969).
21. Walen, W. J., *et al.*, "Microelectrode Determination of Oxygen Profiles in Microbial Slime Systems." *Environ. Sci. Technol.*, **3,** 1297 (1969).
22. Sanders, W. M., III, *et al.*, "Oxygen Microprobe Studies of Microbial Slime Films." *Chem. Eng. Symp. Ser.*, **67,** 69 (1970).
23. Harris, N. P., and Hansford, G. S., "A Study of Substrate Removal in a Microbial Film Reactor." *Water Res.* (G. B.), **10,** 935 (1976).

24. Kehrberger, G. J., "Effect of Recirculation on the Performance of a Trickling Filter." Ph. D. dissertation, Rice Univ., Houston, Tex. (1968).
25. Hoehn, R. C., and Ray, A. D., "Effects of Thickness on Bacterial Film." *J. Water Pollut. Control Fed.*, **45,** 2302 (1973).
26. Fletcher, M., and Floodgate, G. D., "An Electromicroscopic Demonstration of an Acidic Polysaccharide in the Adhesion of a Marine Bacterium to Solid Surfaces." *J. Gen. Microbiol.*, **74,** 325 (1973).
27. Costerton, J. W., *et al.*, "How Bacteria Stick." *Sci. Am.*, **238,** 86 (1978).
28. Bryers, J. D., "Dynamics of Early Biofilm Formation in a Turbulent Flow System." Ph. D. dissertation, Rice Univ., Houston, Tex. (1980).
29. Williams, A. G., and Wimpenny, J. W. T., "Exopolysaccharide Production by *Pseudomonas* NCIB11264 Grown in Continuous Culture." *J. Gen. Microbiol.*, **104,** 47 (1978).
30. Mian, F. A., *et al.*, "Biosynthesis of Exopolysaccharide by *Pseudomonas aeruginosa*." *J. Bacteriol.*, **134,** 418 (1978).
31. Monod, J., "Récherches sur la Croissance des Cultures Bacteriennes." Hermann et cie., Paris, Fr. (1942).
32. Pirt, S. J., "Principles of Microbe and Cell Cultivation." Halsted Press Book, New York, N. Y. (1975).
33. Bryers, J. D., and Characklis, W. G., "A Mathematical Simulation of Microbial Fouling in Water Supply Systems." *Proc. 97th Annu. Am. Water Works Conf.*, Anaheim, Calif. (May 1977).
34. Charcklis, W. G., "Biofilm Development and Destruction." Final Rep., Electric Power Research Institute RP 902-1, Palo Alto, Calif. (1979).
35. Dias, F. F., *et al.*, "Attached Growth of *Sphaerotilus* and Mixed Populations in a Continuous-flow Apparatus." *Appl. Microbiol.*, **16,** 1191 (1968).
36. Picologlou, B. F., *et al.*, "Biofilm Growth and Hydraulic Performance." *J. Hydraul. Div., Proc. Am. Soc. Civ. Eng.*, **106,** 733 (1980).